Chapter 2

State of the art

This chapter tries to contribute to our understanding of the mechanism of shear strength in reinforced concrete beams with or without shear reinforcement. Conceptual models showing the internal forces in a beam are presented, and a historical introduction of different approaches for shear design of reinforced concrete beams is made. Some current code proposals are reviewed both for members with and for those without web reinforcement. The main characteristics of High-Strength Concrete and how they affect the shear response are also discussed.

Main attention is focused on the design of B-regions, as defined by Schlaich et al. (1987). Figure 2.1 shows the distribution of D and B regions, where D stands for 'discontinuity' or 'disturbed', and B stands for 'beam' or 'Bernoulli'. In D regions, the distribution of strains is significantly nonlinear along the depth and strut-and-tie models are particularly relevant. However, in B regions the strain distribution is linear and the response of the concrete member will be principally due to beam action which implies that the lever arm (z) is constant. The other extreme occurs if the tension in the longitudinal reinforcement remains constant and the lever arm varies (Figure 2.2). This occurs if the shear flow cannot be transmitted because the steel is unbounded, or if the transfer of shear flow is prevented by an inclined crack extending from the load to the reactions. In such a case the shear is transferred by arch action.

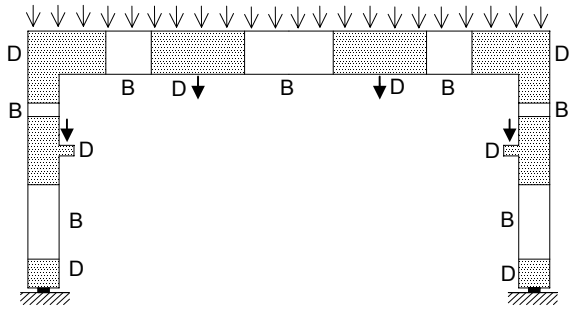

Figure 2.1: B-regions and D-regions (Schlaich et al. ,1987)

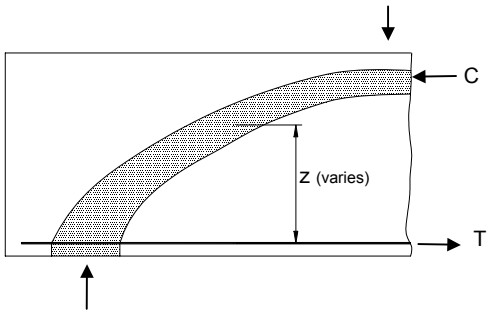

Figure 2.2: Arch action in a beam

2.1 Introduction to High-Strength Concrete (HSC)

In the past decade there has been a rapid growth in interest in high-strength concrete whose compressive strength, f'_c, is higher than 50 MPa. Concretes of strengths up to 100 MPa can be produced not only in precast plants but also in the field, with carefully selected but commonly available cement, sand, and stone, using a very low water-cement ratio and careful quality control during production. The necessary workability is achieved by high-range water-reducing admixtures, the so-called superplasticisers.

The main applications for high-strength *in situ* concrete appear to be in offshore structures, columns for tall buildings, long-span bridges and other highway structures. In precast concrete, applications are mainly in prestressed elements. For instance, the specified concrete strength for the *in situ* columns of the 58-storey Two Union Square Centre in Seattle (1989) was 120 MPa (Figure 2.3). Two pedestrian bridges constructed in Barcelona for the 1992 Olympic Games, shown in Figure 2.4, were the first constructions to be designed and built using HSC in Spain.

Fig. 2.3: Two Union Square Centre, Seattle

Figure 2.4: Montjuïc pedestrian bridge, Barcelona.

Extensive experimentation has greatly improved our understanding of the fundamental behaviour and basic engineering properties of the material. While most of concrete's properties improve as its compressive strength increases, some of its characteristics require special attention. To ensure the safety and serviceability of structural concrete, certain essentially empirical design procedures and equations, based on the characteristics of concretes of much lower strengths, must be re-examined.

The shear capacity of reinforced high-strength concrete beams is an important issue. Provisions for shear design are based mainly on experimentally derived equations. Tests providing the basic data for these equations were conducted on members whose concrete strengths were mainly below 40 MPa. These current approaches will be analysed in this thesis. Section 2.4 introduces the main characteristics of the shear strength of high-strength concrete beams.

The stress-strain behaviour of HSC in uniaxial compression has been reported by many research centres. Figure 2.5 plots the main differences between the stress-strain curves of normal and high-strength concrete, which are:

- a more linear stress-strain relationship up to a higher % of the maximum stress
- a slightly higher strain at the maximum stress
- a steeper shape in the descending part of the curve

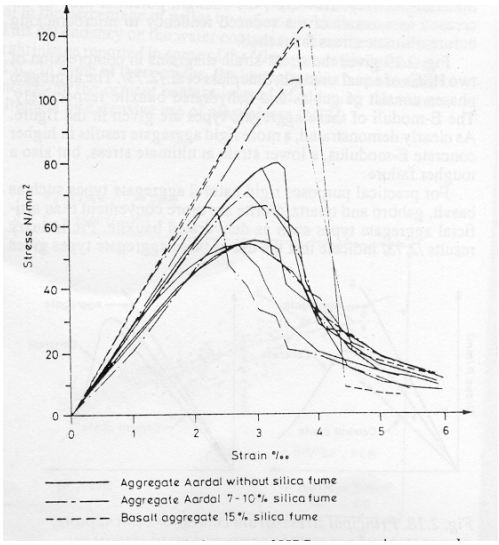

Figure 2.5: Typical stress-strain relationships for high-strength concrete (from FIP/CEB Working Group on HSC, 1990)

As illustrated in Figure 2.6, both cement paste and natural rock aggregates are brittle materials. The concrete made up of these materials has an obvious ductile behaviour. This apparently paradoxical property can be explained as a result of the difference in rigidity that normally exists between the cement paste and the aggregates. This difference will result in stress concentrations in the contact zones. Consequently, at a certain overall stress level, a distributed microcrack pattern will begin to form. As the overall stress increases, an increasing part of the applied energy will be consumed as the crack pattern develops. At this stage, the stress-strain curve will tend to deviate from the linear-elastic course, as shown in the figure. After the ultimate stress level has been reached, the microcrack pattern will provide an efficient internal redistribution of the stress, and hence a tough failure.

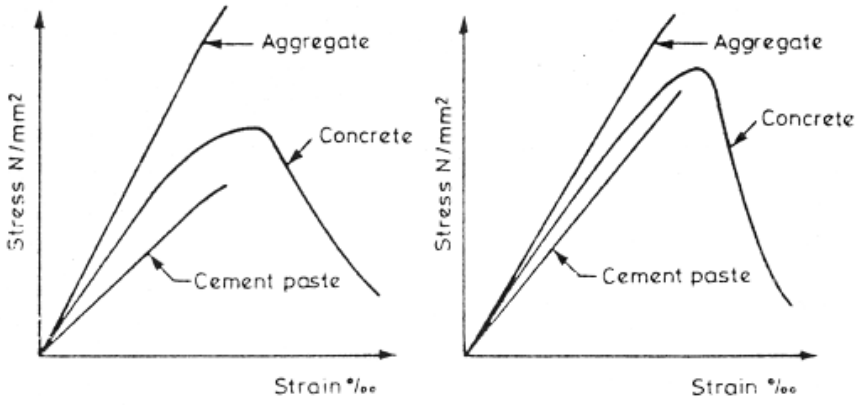

a) Normal strength concrete *b) High-strength concrete*

Figure 2.6: Principal stress-strain curves for cement paste, aggregates and concrete in compression (from FIP/CEB Working Group on HSC, 1990)

The difference in rigidity between cement paste and aggregates is far less in HSC than in normal strength concrete, as illustrated in Figure 2.6. Consequently, the internal stress-distribution is more homogeneous. As the tendency toward early microcracking is reduced, the stress-strain curve becomes more linear. A less developed microcrack pattern also results in a more sudden failure, because the ability to redistribute stress is reduced.

Although the tensile strength of concrete is neglected in calculating the strength of reinforced and prestressed concrete structures, it is generally an important aspect during the development of cracking, and therefore, for the prediction of deformations and the durability of concrete. Other characteristics such as bond and development length of reinforcement and the concrete contribution to the shear and torsion capacities are closely related to the tensile strength of concrete. The tensile strength generally increases along with the compressive strength. However, this increase is not directly proportional to the compressive strength.

2.2 Shear strength in reinforced concrete beams without web reinforcement

2.2.1 Mechanisms of shear transfer

The 1973 ASCE-ACI Committee 426 Report identified the following four mechanisms of shear transfer: shear stresses in uncracked concrete; interface shear transfer, often called “aggregate interlock” or “crack friction”; the dowel action of the longitudinal reinforcing bars; and arch action. The 1998 ASCE-ACI Committee 445 Report highlights a new mechanism, residual tensile stresses, which are transmitted directly across cracks. Opinions vary about the relative importance of each mechanism in the total shear resistance, resulting in different models for members without transverse reinforcement. The forces transferring shear across an inclined crack in a beam without stirrups are illustrated in Figure 2.7.

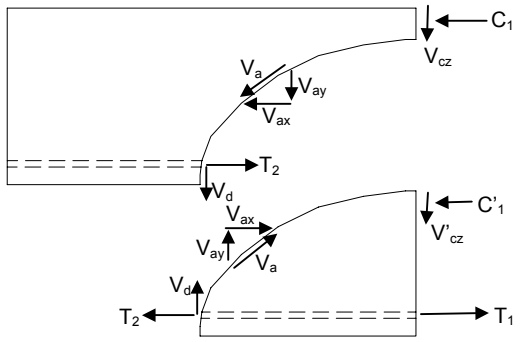

Figure 2.7: Internal forces in a cracked beam without stirrups (adapted from MacGregor and Bartlett 2000)

The shear stresses in uncracked concrete are not a very important mechanism for slender members without axial compression because the depth of the compression zone is relatively small. On the other hand, at locations of maximum moment for less slender beams, much of the shear is resisted in the compression zones, particularly after significant yielding of the longitudinal reinforcement.

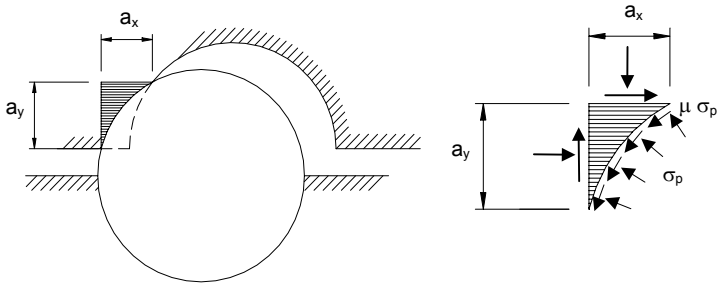

Figure 2.8: Walraven's model of crack friction

Shear transfer in the interface was due primarily to 'aggregate interlock', and hence caused by those aggregates that protruded from the crack surface and provided resistance against slip. However, as cracks go through the aggregate in lightweight and high-strength concrete yet still have the ability to transfer shear, the term 'friction' is more appropriate. The four basic parameters involved are the crack interface shear stress, normal stress, crack width, and crack slip. Walraven (1981) made numerous tests and developed a model that considered the probability that aggregate particles, idealised as spheres, would project from the crack interface (Figure 2.8). As slips develop, the matrix phase deforms plastically, coming into contact with projecting aggregates. The stresses in the contact zones are comprised of a constant pressure, σ_p, and a constant shear, $\mu\sigma_p$. The geometry of the crack surface is described statistically in terms of the

aggregate content of the mix and the probabilities of particles projecting out at different degrees.

Dowel action is not very significant in members without transverse reinforcement, as the maximum shear in a dowel is limited by the tensile strength of the concrete cover supporting the dowel. Nevertheless, it may be significant in members with large amounts of longitudinal reinforcement, particularly when the longitudinal reinforcement is distributed in more than one layer.

The relative importance of the arch action is direct related to the shear span-to-depth ratio, a/d (i.e. the distance from the support to the load over the effective depth). Beams without stirrups, with an a/d ratio of less than 2.5 develop inclined cracks and, after a redistribution of internal forces, are able to carry an additional load due in part to arch action. Figure 2.9 shows how the failure shear strength of a simply-supported reinforced concrete beam loaded with two-point loads changes as the shear span changes. For these series of beams, tested by Kani (1979), the ultimate shear strength was reduced by a factor of about 6 as the a/d ratio increased from 1 to 7. As the beams contained a large amount of longitudinal reinforcement, flexural failures at midspan did not become critical until a shear span-to-depth ratio of about 7. This doctoral dissertation focuses on members whose a/d ratio is over 2.5.

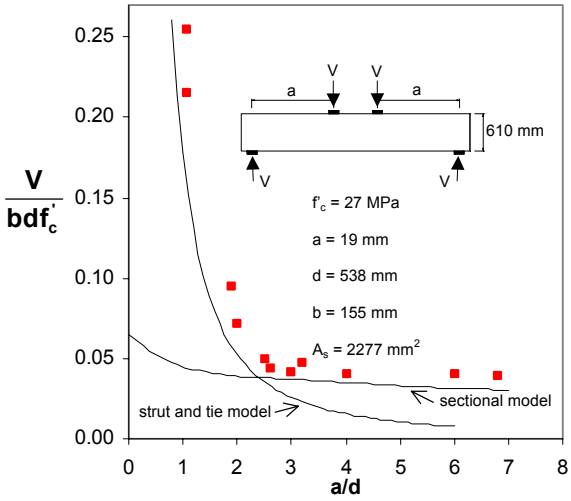

Figure2.9: Predicted and observed strengths of a series of reinforced concrete beams tested by Kani (adapted from Collins and Mitchell 1997)

The basic explanation of residual tensile stresses is that when concrete first cracks, small pieces of concrete bridge the crack and continue to transmit tensile force as long as cracks do not exceed 0.05-0.15 mm in width. The application of Fracture Mechanics to shear design is based on the premise that residual tensile stress is the primary mechanism of shear transfer.

2.2.2 Historical development

Prior to cracking, the maximum shear stress at the web can be calculated by using the traditional theory for homogeneous, elastic and uncracked beams, developed by the 35-year-old Russian railway engineer D.J. Jourawski in 1856 (Collins, 2001):

$$\tau = \frac{V\,Q}{I\,b} \tag{2.1}$$

where I is the moment of inertia of the cross section, Q the first moment about the centroidal axis of the part of the cross-sectional area lying farther from the centroidal axis than the point where the shear stresses are being calculated, and b the width of the member where the stresses are being calculated.

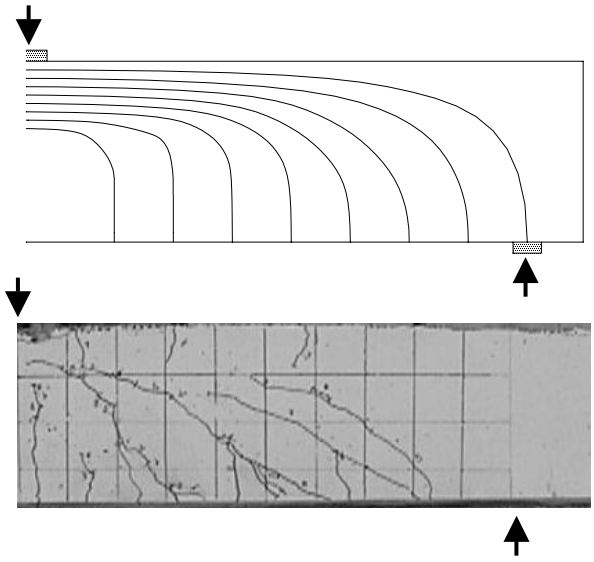

Figure 2.10:Principal compressive stress trajectories in an uncracked beam and photograph of a cracked reinforced concrete beam.

Figure 2.10 shows the principal compressive stress trajectories in an uncracked beam and a photograph of a cracked reinforced concrete beam. Although there is a similarity between the planes of maximum principal tensile stress and the cracking pattern, they

are by no means exactly alike. The flexural cracking, which precedes the inclined cracking, disrupts the elastic stress field to such an extent that inclined cracking occurs at a principal tensile stress, based on the uncracked section, of roughly a third of the tensile strength of the concrete (MacGregor and Bartlett 2000).

In 1902 Mörsch derived the shear stress distribution for a reinforced concrete beam containing flexural cracks. Mörsch predicted that shear stress would reach its maximum value at the neutral axis and would then remain constant from the neutral axis down to the flexural steel (Figure 2.11). The value of this maximum shear stress would be

$$\tau = \frac{V}{b_w z} \tag{2.2}$$

where b_w is the web width and z the flexural lever arm.

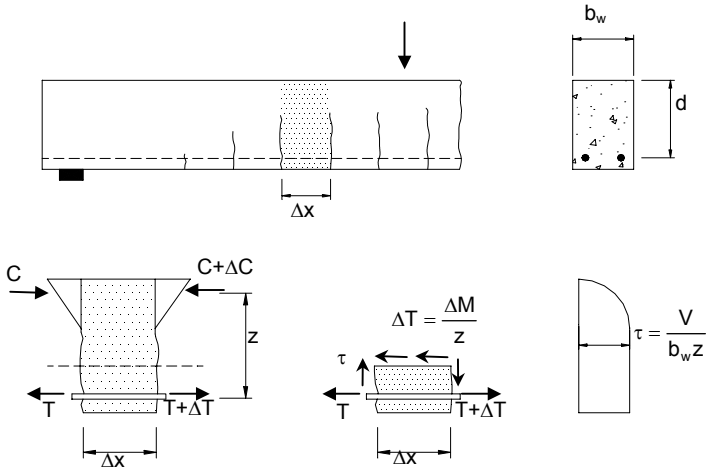

Figure 2.11: Shear stress distribution in a reinforced concrete beam with flexural cracks (adapted from Collins and Mitchell, 1997).

Mörsch recognised that this was a simplification, as some of the transverse force could be resisted by an inclination in the main compression, which would cause the ribs of the concrete between flexural cracks to bend, producing dowel forces in the main steel.

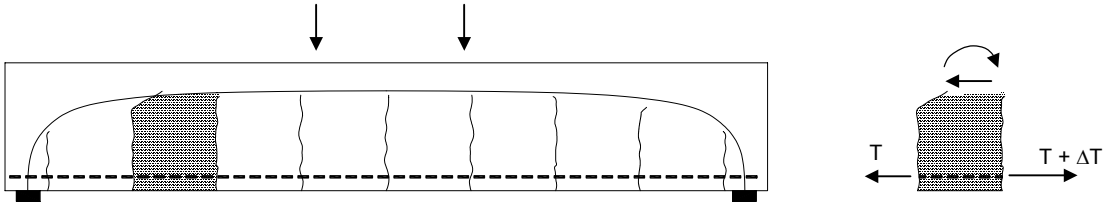

Figure 2.12: Kani's comb model for cracked beams subjected to shear

In 1964, Kani attempted a more realistic approach by addressing the problem of the bending of the 'teeth' of the concrete between flexural cracks. The concrete between two adjacent flexural cracks was considered to be analogous to a tooth in a comb (Figure 2.12). The concrete teeth were assumed to be free cantilevers fixed in the compression zone of the beams and loaded by the horizontal shear from bonded reinforcement. Although this theory did not cover most of the shear transfer mechanisms, it was probably the start of more rational approaches.

Fenwick and Paulay (1968), working with 'tooth' models, pointed out the significance of the forces transferred across cracks in normal beams by crack friction. Taylor (1974), also evaluating Kani's model, found that for normal test beams the components of shear resistance were: compression zone shear (20-40%), crack friction (35-50%) and dowel action (15-25%).

Hamadi and Regan (1980), based on extensive experimental work on interface shear, published an analysis of a tooth model. It was assumed that the cracks were vertical and that their spacing was equal to half the effective depth of a particular beam. Reineck (1991) further developed the tooth model, taking all the shear transfer mechanisms into account, carrying out a full nonlinear calculation including compatibility. Reineck (1991), based on his mechanical model, derived an explicit formula for the ultimate shear force, which matched with the results of the test as well as with those of many empirical formulas.

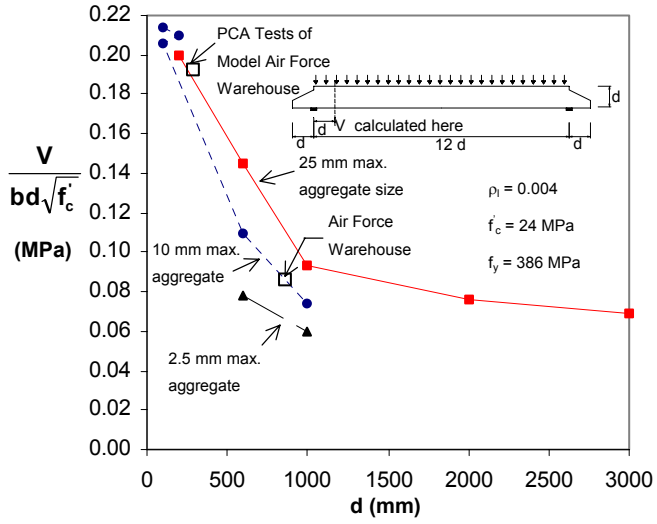

Figure 2.13: Influence of member depth and maximum aggregate size on shear stress at failure (tests by Shioya et al.1989)

Kani raised the size effect subject in 1967, when he demonstrated that as the depth of the beam increases the shear stress at failure decreases. As the depth of the beam increases, the crack widths at points above the main reinforcement tends to increase. Some authors think that this leads to a reduction in the aggregate interlock across the crack, resulting in earlier inclined cracking. Collins and Kuchma (1999) demonstrated that the size effect disappears when beams without stirrups contain well-distributed longitudinal reinforcement. Other authors (Bazant and Kim, 1984) believe that the most important consequence of wider cracks is the reduction in residual tensile stresses. Figure 2.13 shows the results of the tests performed by Shioya et al. (1989). The influence of the concrete compressive strength on the size effect will be discussed in §2.4.3.

The application of simple strut-and-tie models, which have their theoretical basis in the lower-bound theorem of plasticity, requires a minimum amount of distributed reinforcement in all directions to ensure sufficient ductility in order for internal stresses to be redistributed after cracking. However, it is possible to extend this simple strut-and-tie model to members without web reinforcement by using a clearly different approach. Marti (1980) extended the plasticity approach by using a Coulomb-Mohr yield criterion for concrete that includes tensile stresses. In 1987, Schlaich suggested a refined strut-and-tie approach that includes concrete tension ties. Reineck showed that such truss models comply with the tooth model he had proposed.

Empirically derived equations have been very important in the development of procedures used for designing members without transverse reinforcement. The simplest lower-bound average shear stress at diagonal cracking is given by the equation

$$\frac{V_c}{bd} = \tau = \frac{\sqrt{f_c}}{6} \tag{2.3}$$

This well-known ACI equation, basis for the Spanish EH-91 shear provisions, is a reasonable lower bound for smaller slender beams that are not subjected to axial load and have at least 1% longitudinal reinforcement (ACI-ASCE Committee 445, 1998).

However, it may be unconservative for lowly-reinforced members and high-strength concrete members.

The CEB-FIP Model Code (1990) suggests a more sophisticated empirical formula based on Zsutty's (1968, 1971) equation and adding an extra term to account for the size effect (equation 2.4). It should be noted that the formula implicitly includes the concrete safety factor. To disregard this factor, we should use 0.15 as the constant rather than 0.12.

$$\frac{V_c}{b\,d} = 0.12\left(1+\sqrt{\frac{200}{d}}\right)\left(\frac{3\,d}{a_s}\right)^{1/3}\left(100\rho_s f_{ck}\right)^{1/3} - 0.15\sigma_{cd} \qquad (2.4)$$

where σ'_{cd} equals N_d/A_c, N_d being the factored axial force that includes the prestress (tensile positive) force and A_c, the cross sectional area of the concrete

Zsutty's equation took into account the influence of the compression strength of the concrete and the longitudinal reinforcement ratio. When the steel ratio is small, flexural cracks extend higher into the beam and open wider than would be the case with large values of ρ_w.

The MC-90 equation takes the influence of compression force as a factor. However, members without shear reinforcement subjected to large axial compression and shear may fail in a very brittle manner at the first instance of diagonal cracking (Gupta and Collins, 1993). As a result, a conservative approach should be used for those members.

Gastebled and May (2001) recently developed a fracture mechanic model for the flexural-shear failure of reinforced concrete beams without stirrups. They assumed that that the ultimate shear load is reached when a splitting crack at the level of the longitudinal reinforcement starts to propagate. If we adopt the format of the CEB-FIP formula, their equation becomes

$$\frac{V_c}{b\,d} = 0.15\frac{37.41}{\sqrt{d}}\left(\frac{3\,d}{a_s}\right)^{1/3}\left(100\rho_s\right)^{1/6}\left(1-\sqrt{\rho_s}\right)^{2/3} f_c^{0.35} \qquad (2.5)$$

It is worthy a mention that the analytical and the empirical formulas compare very well (Gastebled et al. 2001). However, Gastebled's equation gives more importance to the size effect than the CEB-FIP formula does.

Other different fracture mechanic models have been proposed to account for the fact that a peak tensile stress is near the tip of a crack and a reduced tensile stress (softening) is located in the crack zone. This approach offers a possible explanation for the size effect in shear. Two well known models are the fictitious crack model (Hillerborg et al. 1976), and the crack band model (Bazant and Oh,1983).

The Modified Compression Field Theory (MCFT, Vecchio and Collins 1986) is a general model for the load-deformation behaviour of two-dimensional cracked reinforced concrete subjected to shear. The MCFT, as it will be referred to later in this chapter, is formulated in terms of average stresses and requires an additional check to ensure that the loads resisted by the average stresses can be transmitted across the crack. For members without transverse reinforcement, the local stresses at a crack always control the capacity of the member, and the average stress calculation is used only for estimating the inclination of the critical diagonal crack.

ASCE-ACI Committee 445 (1998) emphasised that, although the refined tooth models and the modified compression field theory take different approaches to the problem, the end result of these two methods is very similar for members without transverse reinforcement. Both methods consider that the ability of diagonal cracks to transfer interface shear stress plays an important role in the determination of the shear strength of members without transverse reinforcement.

2.2.3 Code review

The Spanish EHE-99 Code

The EHE code of practice adopted the CM-90 formula with a minor variation:

$$V_c = \left[0.12\xi\left(100\rho_s f_{ck}\right)^{1/3} - 0.15\sigma'_{cd}\right] b_0 d \qquad (2.6)$$

where, f_{ck} is in MPa and $f_{ck} \leq 60$ MPa,

ξ $= 1 + \sqrt{\frac{200}{d}}$ where d is in mm,

ρ_l $= \frac{A_{sl}}{b_w d} \le 0.02$,

A_{sl} is the area of the anchored tensile reinforcement,

b_0 is the width of the cross-section (in mm),

σ'_{cd} $= N_d/A_c$, N_d being the factored axial force, including the prestress (tensile positive) force and A_c, the cross sectional area of concrete,

V_{Rd} is in Newtons.

The concrete safety factor is also factored into equation 2.6. The constant in that equation (0.12) should be changed to 0.15 to eliminate the safety factor from the equation.

Eurocode 2: April 2002 Final Draft

The final version of the new draft of Eurocode 2 presents a different shear procedure than its predecessor. It is based, with some variations, on the MC-90 equation. The design value for the shear resistance in non-prestressed members not requiring design shear reinforcement is given by:

$$V_{Rd,c} = \left[\frac{0.18}{\gamma_c} k (100 \rho_l f_{ck})^{1/3} + 0.15 \sigma_{cp} \right] b_w d \tag{2.7}$$

with a minimum of

$$V_{Rd,min} = \left[0.035 k^{3/2} f_{ck}^{1/2} \right] b_w d \tag{2.8}$$

where,

f_{ck} is in MPa and $f_{ck} \le 100\ MPa$,

k $= 1 + \sqrt{\frac{200}{d}} \le 2.0$, where d is in mm,

ρ_l $= \frac{A_{sl}}{b_w d} \le 0.02$,

A_{sl} is the area of the anchored tensile reinforcement,

b_w is the smallest width of the cross-section in the tensile area (in mm),

σ_{cp} $= N_{Ed}/A_c < 0.2\, f_{cd}$ (MPa). N_{Ed} is the axial force in the cross-section due to loading or presstressing in Newtons ($N_{Ed} > 0$ for compression). The influence of imposed deformations on N_E can be ignored. A_c is the area of the concrete cross section (mm^2).

V_{Rd} is in Newtons.

AASHTO LRFD 2000

The AASHTO-LRFD shear design procedure is based on the modified compression field theory. The nominal shear resistance for a non-prestressed member without shear reinforcement is given by:

$$V_c = \beta\sqrt{f'_c}\, b_v d_v \tag{2.9}$$

the values of β and θ, depend on the equivalent crack spacing parameter, s_{xe}, where

$$s_{xe} = \frac{35}{a + 16} s_x \tag{2.10}$$

where a is the maximum aggregate size, and s_x is the crack spacing parameter as defined in Figure 2.14.

The longitudinal strain in the web, ε_x, can be derived from the longitudinal strain in the flexural tension flange, ε_t, where

$$\varepsilon_t = \frac{\frac{M_f}{d_v} + V_f - \phi_p V_p + 0.5 N_f - A_p f_{p0}}{E_s A_s + E_p A_p} \tag{2.11}$$

and f_{p0} can be taken to be $0.7 f_{pu}$ at typical levels of prestress. For members without stirrups ε_x can be taken to be ε_t (see Figure 2.14).

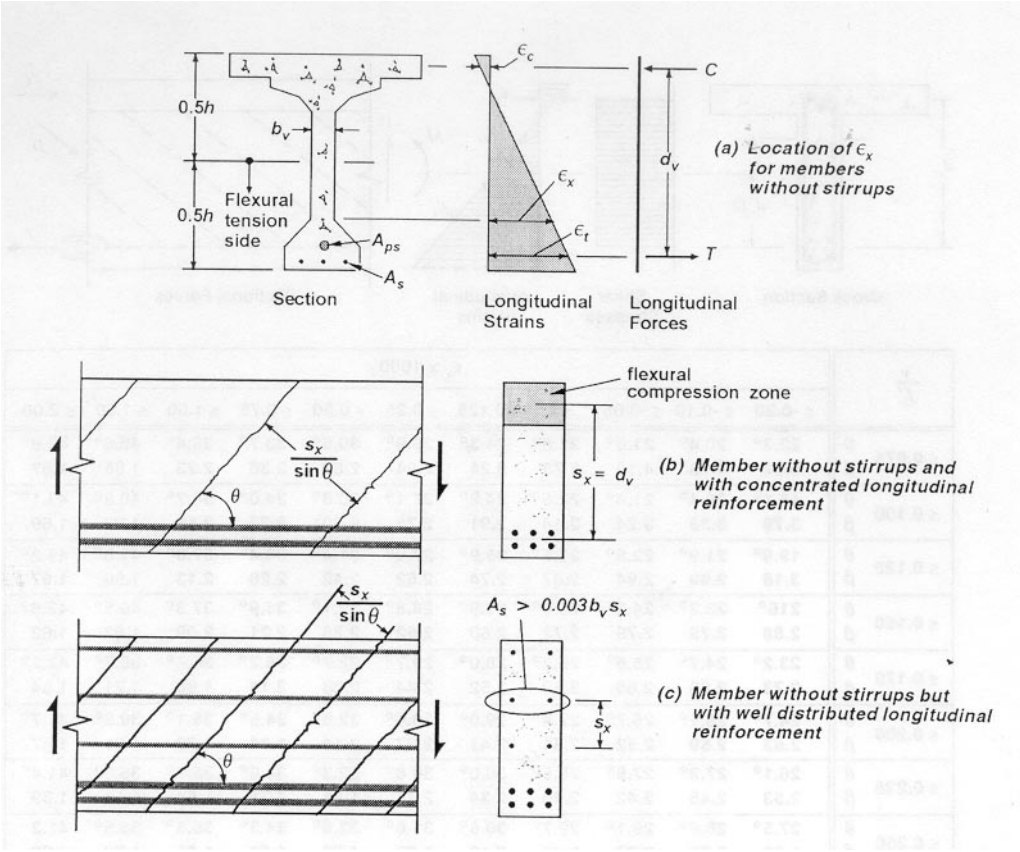

		$\varepsilon_x \times 1000$							
s_z		≤ 0.00	≤ 0.125	≤ 0.25	≤ 0.50	≤ 0.75	≤ 1.00	≤ 1.50	≤ 2.00
≤ 125	β	0.428	0.366	0.325	0.271	0.238	0.214	0.184	0.163
	θ	26.4	27.7	28.9	30.9	32.4	33.7	35.6	37.2
≤ 250	β	0.406	0.336	0.292	0.239	0.208	0.185	0.156	0.137
	θ	29.3	31.6	33.5	36.3	38.4	40.1	42.7	44.7
≤ 375	β	0.393	0.317	0.272	0.219	0.188	0.167	0.140	0.121
	θ	31.1	34.1	36.5	39.9	42.4	44.4	47.4	49.7
≤ 500	β	0.383	0.303	0.257	0.204	0.174	0.154	0.126	0.109
	θ	32.3	36	38.8	42.7	45.5	47.6	50.9	53.4
≤ 750	β	0.368	0.282	0.234	0.182	0.153	0.133	0.108	0.091
	θ	34.2	38.9	42.3	46.9	50.1	52.6	56.3	59
≤ 1000	β	0.337	0.266	0.218	0.166	0.138	0.119	0.095	0.079
	θ	36.6	41.1	45	50.2	53.7	56.3	60.2	63
≤ 1500	β	0.291	0.242	0.193	0.143	0.116	0.098	0.076	0.062
	θ	40.8	44.5	49.2	55.1	58.9	61.8	65.8	68.6
≤ 2000	β	0.257	0.225	0.175	0.126	0.100	0.084	0.063	0.051
	θ	44.3	47.1	52.3	58.7	62.8	65.7	69.7	72.4

Figure 2.14: Values of β and θ for sections without shear reinforcement.

ACI Code 318-99

The ACI code of practice presents two different procedures for calculating the failure shear strength for concrete beams without shear reinforcement. The simplified method, equation 11-3, is as follows:

$$V_c = \left(\frac{\sqrt{f'_c}}{6} \right) b_w d \tag{2.12}$$

The second procedure, equation 11-5, applies for those members whose a/d ≥ 1.4:

$$V_c = \left(\sqrt{f'_c} + 120 \rho_w \frac{d}{a} \right) \frac{b_w d}{7} \leq 0.3 \sqrt{f'_c} b_w d \tag{2.13}$$

where $f'_c < 70\ MPa$, and all the other variables are as defined previously.

2.3 Members with web reinforcement

2.3.1 Forces in members with web reinforcement

Ideally, the purpose of web reinforcement is to ensure that shear failure does not occur and that the full flexural capacity can be used. Prior to inclined cracking, the strain in the stirrups is equal to the corresponding strain in the concrete and, therefore, the stress in the stirrups prior to inclined cracking will be relatively small. Stirrups do not prevent inclined cracks from forming as they come into play only after cracks have formed.

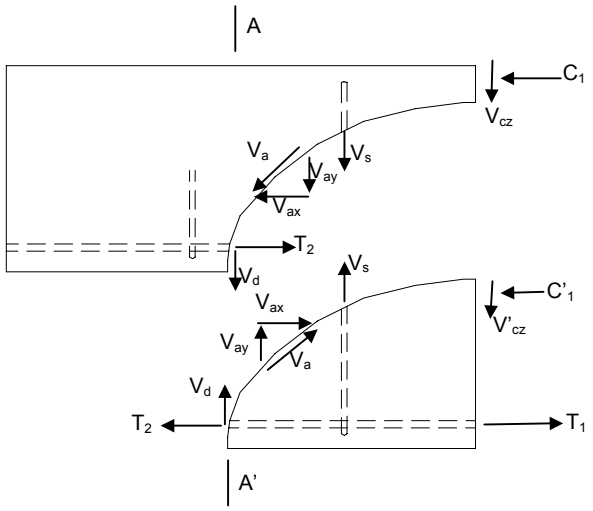

Figure 2.15: Internal forces in a cracked beam with stirrups (adapted from MacGregor et al. 2000).

Figure 2.15 shows the forces in a beam with stirrups after the development of an inclined crack. The shear transferred by tension in the stirrups is V_s. Since V_s does not

disappear when the crack opens, to verify equilibrium there will always be a compression force, C'_1, and a shear force, V'_{cz}, acting on the part of the beam below the crack. Thus, T_2 will be less than T_1 and the difference will depend on the amount of web reinforcement. However, the force T_2 will be larger than $T = M/z$ based on the moment at A-A'.

2.3.2 Historical development

In the early 20th century, truss models were used as conceptual tools in the analysis and design of reinforced concrete beams. Ritter (1899) and Mörsch (1902) postulated independently that after a reinforced concrete beam cracks due to diagonal tensions stresses, it can ideally be thought of as a parallel chord truss with compression diagonals inclined at 45° with respect to the longitudinal axis of the beam. Several years later, Mörsch (1920,1922) introduced the use of truss models for torsion. In these truss models, in which the contribution of the concrete in tension is neglected, the diagonal compressive concrete stresses push apart the top and bottom faces of the beam, while the tensile stresses in the stirrups pull them together (Figures 2.16 and 2.17). Equilibrium requires these two effects to be equal. According to the 45° truss model, the shear capacity is reached when the stirrups yield and will correspond to a shear stress of

$$\tau = \frac{A_v f_y}{b_w s} = \rho_v f_y \tag{2.14}$$

where A_v is the area of the transverse reinforcement, s the spacing of the transverse reinforcement, f_y the steel yielding stress and b_w the web width.

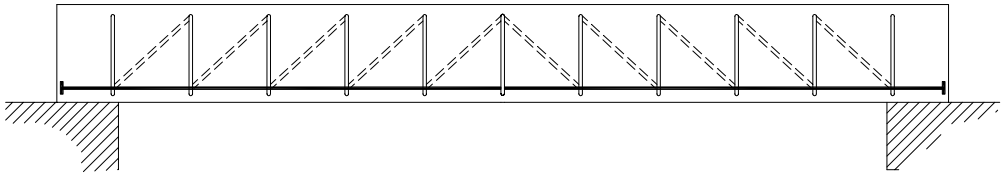

Figure 2.16: Ritter's truss model.

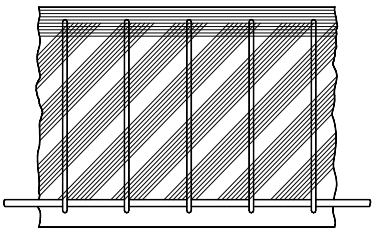

Figure 2.17: Mörsch truss analogy.

In the United States an extra term was added to improve correlation with test results, but it was never explained in physical terms. It has generally been taken to be the strength of a similar beam without stirrups but, in light of the very different ultimate load behaviour in each case, this equation is physically misleading (Regan, 1993). From 1921 to 1951 each new edition provided somewhat less conservative design procedures (ASCE-ACI Committee 445), even though Talbot (1909) had pointed out that the value of the shear stress at failure varied with the amount of reinforcement, the relative length of the beam and the quality and the strength of the concrete in addition to other factors that affect the stiffness of the beam. However, ACI 318-51 only specified that web reinforcement must be provided for the excess shear if the shear stress at service loads exceeded $0.03 \cdot f'_c$.

Figure 2.18: Wilkins Air Force Depot in Shelby, Ohio.

The August 1955 brittle shear failure of beams in a warehouse at Wilkins Air Force Depot in Shelby, Ohio, (Elstner et al. 1957, Anderson 1957) brought traditional shear design procedures into question. The collapse was caused by the shear failure of 914 mm deep beams that did not contain stirrups at the location of failure and only had 0.45 percent of longitudinal reinforcement. The beams failed at a shear stress of less than 0.5 MPa, a low working stress compared with that obtained using the ACI provisions of that days. Experiments (Elstner et al. 1957) conducted at the Portland Cement Association on 305 mm deep beams indicated that the beams could resist a shear stress of about 1.0 MPa prior to failure. However, application of an axial tensile stress of about 1.4 MPa reduced the shear capacity by about 50 percent. It was concluded that tensile stresses caused by the restraint of shrinkage and thermal movements were the reason for the beams' failure at such low shear stresses. However, as can be seen in Figure 2.13, the size effect, which was the real reason for the failure, was not taken into consideration.

Shear/compression theories started to be developed in the 1950s. The idea behind them is that beam failure is caused by crushing of the concrete compression zones, the depth of which has been reduced by a shear crack. The limiting compressive stresses may also be reduced by the effects of shear in the compression zone. In 1958, Walther proposed what was probably the best known of these theories. However, the complexity of this theory resulted in the impossibility of finding an explicit solution.

The early work by Ritter and Mörsch received new impetus in the period during the three decades from 1960 to 1980. In Stuttgart, Leonhardt and Walther (1961) carried out an extensive experimental campaign on beams failing in shear and developed a model that combined the beam and the arch effects. It was shown that these two resistant mechanisms interact and that the relative importance of each one varies depending on the slenderness of the beam.

Attention was also focused on truss models with diagonals having a variable angle of inclination (§2.3.3) as a viable model for shear and torsion in reinforced and prestressed concrete beams (Kupfer, 1964). Kupfer provided a solution for the inclination of the diagonal cracks by considering linearly elastic members and ignoring the concrete tensile strength. Further development of plasticity theories extended the applicability of the model to non-yielding domains (Nielsen and Braestrup, 1975). Schlaich et al. (1987)

extended the truss model for beams with uniformly inclined diagonals. This approach is particularly relevant in D-regions where the distribution of strains is significantly nonlinear along the depth.

Modified truss models are used in more recent design codes. For example, ACI Building Code 318-99 still adds a concrete contribution term to the shear reinforcement capacity obtained, assuming a 45° truss. Another procedure involves the use of a truss with a variable angle of inclination for the diagonals. The inclination of the truss diagonals is allowed to deviate from 45° within certain limits baed on the theory of plasticity. The CEB-FIP model code for concrete structures (1978), and many codes of practice derived from it, adopted a combination of the variable-angle truss and concrete contribution.

Mitchell and Collins (1974) developed the diagonal Compression Field Theory for members subjected to pure torsion. The Compression Field Theory (Collins 1978) and the Modified Compression Field Theory (MCFT, Vecchio and Collins 1986) extended the first theory, dating from 1974, to shear. The MCFT (Figure 2.19) is a further enhancement of the CFT that accounts for the influence of the tensile stresses in the cracked concrete. They take into account the overall load/deformation responses of elements in which the reinforcement acts in uniaxial tension and the concrete works in biaxial tension/compression. The principal stresses and strains in the concrete are assumed to be coincident. The equilibrium equations, the compatibility relationships, the reinforcement stress-strain relationships, and the stress-strain relationships for the cracked concrete in compression and tension enable one to determine the average stresses, the average strains, and the angle θ for any load level up to failure. Failure of the reinforced concrete element may not be governed by average stresses, but rather by local stresses that occur at a crack. This so-called crack check is a critical part of the MCFT and the theories derived from it. The crack check involves limiting the average principal tensile stress in the concrete to a maximum allowable value determined by considering the steel stress at a crack and the ability of the crack surface to resist shear stresses.

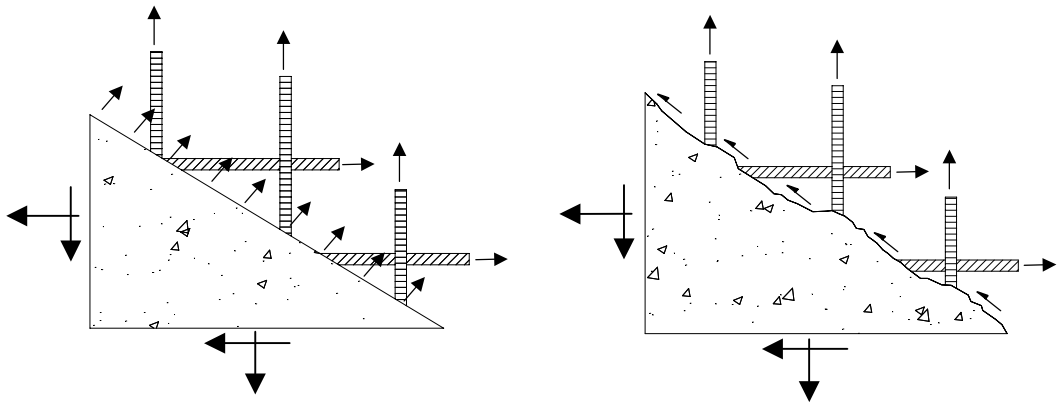

a) Average stresses *b) Stresses at a crack*

Figure 2.19: MCFT: average stresses and stresses at a crack

Hsu and his colleagues from the University of Houston (Berlabi and Hsu 1994, 1995) presented the Rotating-Angle Softened-Truss Model (RA-STM). Like the MFCT, this method assumes that the inclination of the principal stress direction, θ, coincides with the principal strain direction. For typical elements, θ will decrease as the shear is increased, hence the name 'rotating angle'. Pang and Hsu (1995) limited the applicability of the rotating-angle model to situations in which the rotating angle does not deviate from the fixed angle by more than 12°. Outside this range they recommend the use of a fixed angle model where it is assumed (Pang and Hsu, 1996) that shear cracks are parallel to the principal direction of compressive stress as defined by the applied loads.

The Disturbed Stress Field Model (DSFM), developed by Vecchio (Vecchio 2000, Vecchio 2001) as an extension of the MCFT, explicitly incorporates rigid slipping along crack surfaces into the compatibility relations for the element. This allows for a divergence of the angles of inclination of average principal stress and apparent average principal strain in the concrete. The model represents cracks as gradually rotating, but typically lagging behind the reorientation of the principal strains. Vecchio et al. (2001) concludes that 'the corroboration studies for the DSFM also reaffirmed the strength of the MCFT as a simple model providing good accuracy over a wide range of conditions. Although the MCFT's assumption of coaxiality of stresses and strains is shown to have some fault [..] its influence on predicted behaviour is minor in most cases'.

2.3.3 Truss models

Truss models are provide an excellent conceptual model for showing the forces that exist in a cracked concrete beam. The 45° Mörsch model can be made more accurate by accounting for the fact that θ is typically less than 45°. Figure 2.19 summarises the equilibrium conditions for the variable-angle truss-model.

The required magnitude for the principal compressive stresses, f_2, can be derived from the free-body diagram shown in Figure 2.20:

$$f_2 = \frac{V}{b_w z}\left(\tan\theta + \cot\theta\right) \tag{2.15}$$

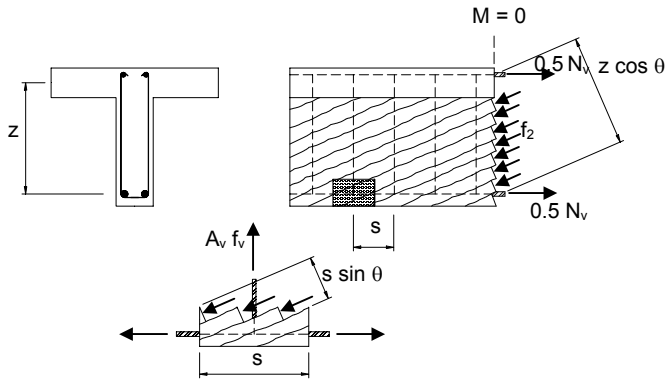

Figure 2.20: Equilibrium conditions for a variable-angle truss (adapted from Collins and Mitchell, 1991).

The tensile force in the longitudinal reinforcement due to shear forces is

$$N_v = V \cot\theta \tag{2.16}$$

The compressive stresses, f_2, in the web tend to cause the top and bottom flanges to separate. To prevent this from happening, the tensile force of the stirrups must be equal to the vertical component of the compression force in the web:

$$\frac{A_v f_y}{s} = \frac{V}{z}\tan\theta \tag{2.17}$$

The equilibrium equations shown above are insufficient, however, for gauging the stresses caused by a given shear in a beam. There are four unknowns (i.e., the principal

compressive stress, the tensile force in the longitudinal reinforcement, the stress in the stirrups and the inclination, θ, of the principal compressive stresses).

In the traditional truss model the failure shear strength of a beam is determined using an equilibrium equation by assuming that at failure the stirrups yield and that $\theta = 45°$. Otherwise, it can be assumed a compressive stress, f_2, in the concrete at failure and then find V and θ. Alternatively, it could be assumed that, at failure, both the longitudinal reinforcement and the stirrups yield, and then determine V and θ from this. These approaches, which consider the mechanisms of failure, are referred to as plasticity methods. Nielsen (1984) summarised these methods.

The EHE code of practice assumes that a concrete contribution, V_c, can be added to the steel contribution. This contribution is taken to be approximately 85% of the cracking shear strength of a beam without stirrups. It should be emphasised that taking V_c to be equal to the shear at inclined cracking is approximately true if it is assumed that the horizontal projection of the inclined crack is d (MacGregor et. al, 2000). If a flatter crack is used, so that $z \cdot cot\theta$ is greater than d, a smaller value of V_c must be used. For values of θ approaching 30°, used in the plastic truss model, V_c approaches zero, as represented in the EHE Code by the constant β, by which the concrete contribution, V_c, is multiplied:

$$V = V_s + \beta V_c \tag{2.18}$$

For non-prestressed members without axial force β equals 1 if θ is taken to be 45°. If $cot\ \theta$ is assumed to be equal to 2 (thus $\theta \approx 26.6°$), then $\beta = 0$.

From a truss model it is possible to identify the different shear failure modes that may cause the failure of a beam:

Failure due to the stirrups yielding. Assuming that all the stirrups crossing a crack yield at failure, the shear resisted by the stirrups is

$$V_s = \frac{A_v f_y d}{s} \tag{2.19}$$

However, stirrups are unable to resist shear unless they are crossed by an inclined crack. It is possible for a 45° crack to cross the web without intersecting a stirrup if the stirrup spacing exceeds *d*. Therefore, the maximum stirrup spacing should be *d* or less.

In a wide beam with stirrups around the perimeter, the diagonal compressive stresses in the web tend to be supported by the longitudinal bars in the corners, as shown in Figure 2.21. The situation is improved if there are more than two stirrup legs. The CEB-FIP 1990 suggests that the maximum transverse spacing of the stirrup legs should be limited to the smaller of 2d/3 or 800 mm. Serna et al. (2000) concluded that for wide beams the use of two leg stirrups should be banned and that the maximum distance in the transverse direction between legs should be limited to *d*.

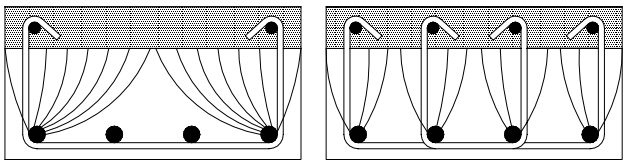

Figure 2.21: Flow of the diagonal compressive force in cross-sections of wide beams. Adapted from MacGregor et al. (2000).

Equation 2.19 is based on the assumption that the stirrups will yield before failure. This is true only if the stirrups are well anchored. Because the available development length between the inclined crack and the end of the stirrup can be very short, the use of small diameter stirrups as well as hoops with the adequate geometry is recommended.

Moreover, wide cracks in beams are unsightly and may allow water to penetrate the beam, possibly causing the stirrups to corrode. Crack width is smaller with very closely-spaced small-diameter stirrups than with widely-spaced large-diameter stirrups. The use of horizontal steel distributed near the faces of beam webs is also effective in reducing crack width. Some codes, such as the Canada's CSA-94, attempt to guard against excessive crack widths by limiting the maximum shear that can be transmitted by stirrups to

$$V_{s,max} = 0.8\phi_c \sqrt{f_c'} b_w d \tag{2.20}$$

where $\phi_c = 0.60$ is the concrete safety factor.

Shear failure due to crushing of the web. As indicated earlier and shown in equation 2.15, compression stresses exist in the web of a beam. In very thin-walled beams, these may lead to crushing of the web. In predicting the shear strength of beams using variable-angle truss models, it is necessary to use an 'effective' concrete compressive strength smaller in value than the cylinder crushing stress. A value of $0.6f_c'$ is frequently recommended.

Shear failure initiated by failure of the tension chord. The longitudinal component of the diagonal compressive force must be counteracted by an equal tensile force in the longitudinal reinforcement. This tension increase may cause the longitudinal reinforcement to yield, producing the failure of the beam. The truss analogy shows that the force in the longitudinal tensile reinforcement at a given point in the shear span is a function of the moment at a section located approximately $d_v cot\theta$ closer to the nearest section of maximum moment.

2.3.4 Modified Compression Field Theory

Mörsch (1922) stated that it was absolutely impossible to mathematically determine the slope of the secondary inclined cracks to design the stirrups. The German engineer Wagner (1929), however, solved an analogous problem when dealing with the post-buckling shear resistance of thin-webbed metal girders. Wagner assumed that after the thin metal skin buckled, it could continue to carry shear by a field of diagonal tension, supposing that it was stiffened by transverse frames and longitudinal stringers. He assumed that the angle of inclination of the diagonal tensile stresses in the buckled thin metal skin would coincide with the angle of inclination of the principal tensile strain as determined from the compatibility of the deformation of the skin, the transverse frames and the longitudinal stringers.

The compression field approaches also determine the angle θ by considering the compatibility of the deformations of the transverse reinforcement, the longitudinal

reinforcement, and the diagonally stressed concrete. Therefore, these methods satisfy equilibrium, strain compatibility and stress-strain relationships.

The first method for determining θ that was applicable over the full loading range and based on Wagner's procedure was developed for members in torsion by Mitchell and Collins (1974). Further developments led to the Modified Compression Field Theory (Vecchio and Collins, 1986).

The MCFT is a general model for the load-deformation behaviour of two-dimensional cracked reinforced concrete subjected to shear. As discussed earlier, it models concrete considering concrete stresses in the principal directions summed with reinforcing stresses assumed to be only axial. The concrete stress-strain behaviour in compression and tension was derived originally from tests performed by Vecchio (Vecchio and Collins, 1982).

The key assumption the MFCT uses to simplify is that the principal strain directions coincide with the principal stress directions. This assumption is confirmed by experimental measurements, which show that the principal directions of stress and strain are parallel within ±10º.

Concrete struts are also at a shallower angle than cracks, and the compressive stress field must be transferred across the cracks, which causes the concrete strength to be reduced from its uncracked state and inducing shear stress across the crack faces. This produces tensile stresses in the cracked concrete.

Local stresses in both the concrete and the reinforcement are recognised to vary from point to point in the cracked concrete, with high reinforcement stresses but low concrete tensile stresses taking place at the location of the crack. In the MCFT the compatibility conditions relating the strains in the cracked concrete with the strains in the reinforcement are expressed in terms of average strains, where the strains are measured over base lengths that are greater than the crack spacing. The equilibrium conditions, which relate the concrete stresses and the reinforcement stresses to the applied loads, are also expressed in terms of average stresses.

Similarly, the strains used for the stress-strain relationships are average strains, that is, they consider together the combined effects of local strains at cracks, strains between cracks, bond-slip, and crack slip. The calculated stresses are also average stresses in that they implicitly encompass the stresses between cracks, stresses at cracks, interface shear on cracks and dowel action. In this model, the cracked concrete in reinforced concrete is treated as a new material with empirically defined stress-strain behaviour. This behaviour can differ from the traditional stress-strain curve of a cylinder, for example.

The equilibrium equations, the compatibility relationships, the reinforcement stress-strain relationships, and the stress-strain relationships for the cracked concrete in compression and tension enable the average stresses, the average strains, and the angle θ to be determined for any load level up to failure.

Failure of reinforced concrete element may be governed not by average stresses, but rather by the local stresses occurring at a crack. A so-called 'crack check' is a critical part of the MCFT and the theories derived from it. The crack check involves limiting the average principal tensile stress in the concrete to a maximum allowable value determined by considering the steel stress at the crack and the ability of the crack surface to resist shear stresses.

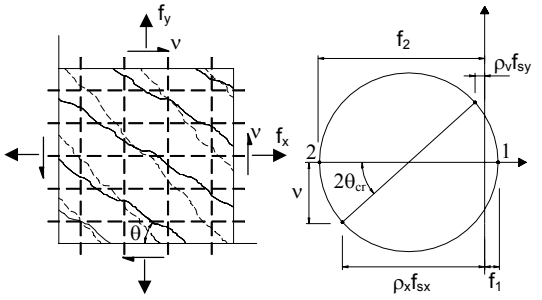

Fig. 2.22: Equilibrium in terms of average stresses

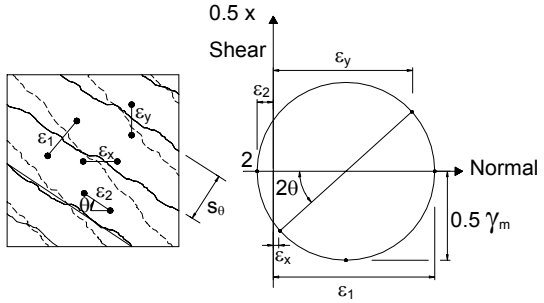

Fig 2.23: Compatibility in terms of average strains

Figure 2.22 is used to establish the equations of equilibrium between cracks. Shear in the section is resisted by the diagonal compressive stresses, f_2, together with the diagonal tensile stresses, f_1. The tensile stresses vary from 0 at the cracks to a maximum between cracks. As has been mentioned, the average value is used in the equilibrium formula.

$$\rho_y f_{sy} = f_y + v \tan\theta - f_1 \tag{2.21}$$

$$\rho_x f_{sx} = f_x + v \cot\theta - f_1 \tag{2.22}$$

$$f_2 = v(\tan\theta + \cot\theta) - f_1 \tag{2.23}$$

The compatibility equations for the average concrete strains are established using the geometrical transformations represented by Mohr's Circle of Strain as shown in Figure 2.23.

$$\varepsilon_x = (\varepsilon_1 \tan^2\theta + \varepsilon_2)/(1 + \tan^2\theta) \tag{2.24}$$

$$\varepsilon_y = (\varepsilon_1 + \varepsilon_2 \tan^2\theta)/(1 + \tan^2\theta) \tag{2.25}$$

$$\gamma_{xy} = 2(\varepsilon_x - \varepsilon_2)/\tan\theta \tag{2.26}$$

$$\tan^2\theta = (\varepsilon_x - \varepsilon_2)/(\varepsilon_y - \varepsilon_2) \tag{2.27}$$

The reinforcement stress-strain relationship is a typical bilinear diagram:

$$f_{sx} = E_s \varepsilon_x \le f_{x\,yield} \tag{2.28}$$

$$f_{sy} = E_s \varepsilon_y \le f_{y\,yield} \tag{2.29}$$

The concrete web acts not only in compression in direction 2, but also in tension in direction 1. Therefore, the following average stress-strain relationships, based on Vecchio's experiments (Vecchio and Collins, 1982), are adopted:

$$f_2 = \frac{f'_c}{0.8 + 170\varepsilon_1}\left[2\frac{\varepsilon_2}{\varepsilon'_c} - \left(\frac{\varepsilon_2}{\varepsilon'_c}\right)^2\right] \tag{2.30}$$

$$f_1 = \frac{f_{cr}}{1 + \sqrt{500\varepsilon_1}} \tag{2.31}$$

where f_{cr} is the cracking strength of concrete. Figures 2.24 and 2.25 represent the above equations.

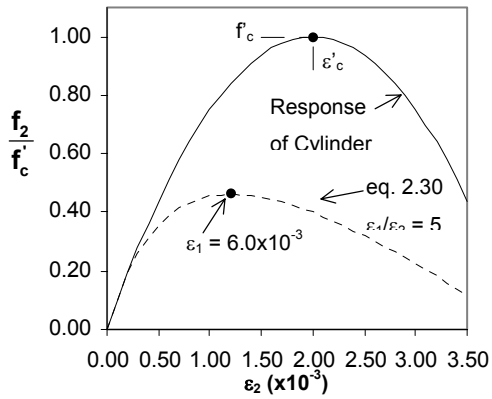

Fig. 2.24: Compressive stress-strain relationships for cracked concrete

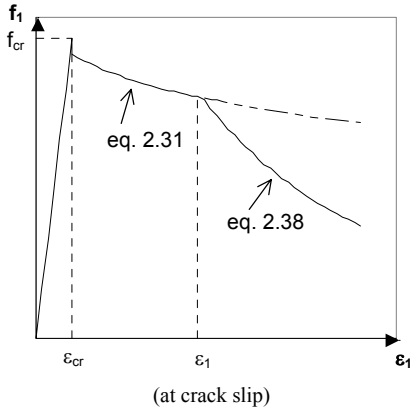

Fig. 2.25: Average stress-strain relationship for concrete in tension

In checking the conditions at a crack, the actual complex crack pattern is idealised as a series of parallel cracks, all occurring at an angle θ to the longitudinal reinforcement and spaced a distance s_θ apart. The reinforcement stresses at a crack, deduced from Figure 2.26, can be determined by the equations

$$\rho_x f_{sxcr} = f_x + v\cot\theta + v_{ci}\cot\theta \tag{2.32}$$

$$\rho_y f_{sycr} = f_y + v\tan\theta - v_{ci}\tan\theta \tag{2.33}$$

The ability of the crack interface to transmit the shear stress, v_{ci}, depends on the crack width, ω. The limiting value of v_{ci} proposed by Vecchio and Collins is

$$v_{ci} \le \frac{0.18\sqrt{f'_c}}{0.3 + \dfrac{24\omega}{a+16}} \tag{2.34}$$

where a is the maximum aggregate size in mm.

This equation, based on Walraven's (1981) experiments, was performed on various concretes whose cube strengths were 13, 37, and 59 MPa. Nevertheless, as the aggregate may fracture for high f'_c, and for low f'_c fracture goes around the aggregates, this formula will require further investigation (Duthinh et al., 1996),.

The above formula requires an estimation of the crack width, taken to be the crack spacing multiplied by the principal tensile strain, ε_1:

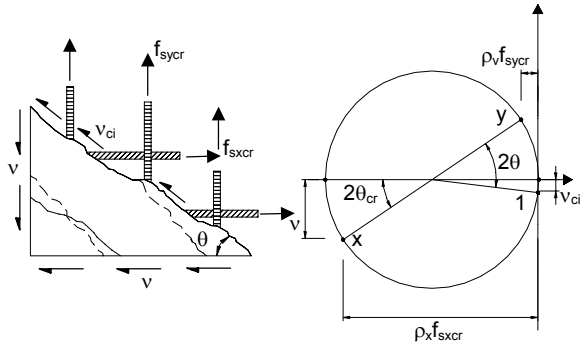

Fig. 2.26: Equilibrium in terms of local stresses at a crack

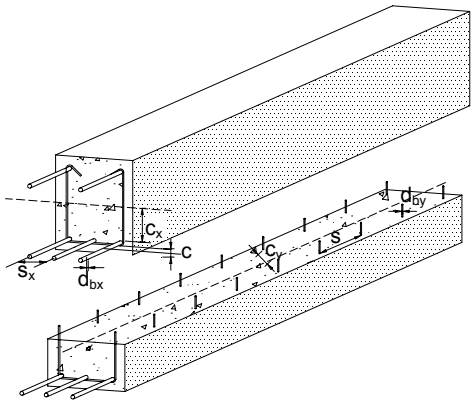

Fig. 2.27: Parameters influencing crack spacing (Collins and Mitchell, 1997)

$$\omega = \varepsilon_1 s_{m\theta} \tag{2.35}$$

$$s_{m\theta} = \frac{1}{\frac{\sin\theta}{s_{mx}} + \frac{\cos\theta}{s_{mv}}} \tag{2.36}$$

Finally, crack spacing, s_{mx} and s_{mv} are estimated using the formulas given by the CEB-FIP Model Code (1990)

$$s_{mx} = 2\left(c_x + \frac{s_x}{10}\right) + 0.25 k_1 \frac{d_{bx}}{\rho_x} \tag{2.37a}$$

$$s_{my} = 2\left(c_y + \frac{s}{10}\right) + 0.25 k_1 \frac{d_{by}}{\rho_y} \tag{2.37b}$$

where d_b = bar diameter,

c = distance to reinforcement,

s = bar spacing,

ρ_y = $A_v/(b_w s)$,

ρ_x = A_x/A_c, and

k_1 = 0.40 for deformed bars or 0.8 for plain bars..

At high loads, the average strain of the stirrups, ε_y, will typically exceed the yield strain of the reinforcement. In this situation, both f_{sy} in equation 2.21 and f_{sycr} in 2.33 will equal the yield stress in the stirrups. Equating the right-hand sides of these two equations and substituting for ν_{ci} from equation 2.34 gives

$$f_1 \le \frac{0.18\sqrt{f_c'}\tan\theta}{0.3 + \frac{24\omega}{a+16}} \tag{2.38}$$

Although in this chapter the full analytical model has been described, there are few simplified methods based on the MCFT that have been adopted in a number of codes (Canada, Norway, and in the AASHTO LRFD).

2.3.5 Truss Model vs. Modified Compression Field Theory

The Modified Compression Field Theory can be explained as a truss model in which the shear strength is the sum of the steel and concrete contributions. The main difference from a classic truss model with concrete contribution is that the concrete contribution in the MCFT is the vertical component of the shear stress transferred across the crack, υ_{ci} (Figure 2.28), and not the diagonal cracking strength:

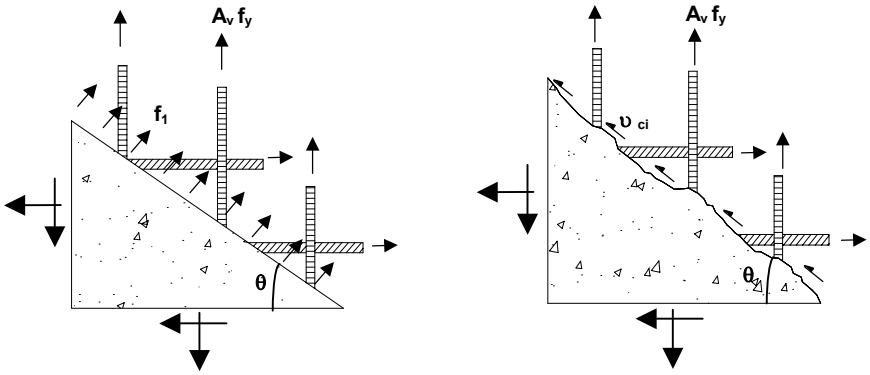

Figure 2.28: Average stresses and stresses at a crack.

$$V = V_c + V_s \tag{2.39}$$

$$V_s = \frac{A_v}{s} f_y d_v \cot g\theta \tag{2.40}$$

$$V_c = \upsilon_{ci} b_w d_v \tag{2.41}$$

Figure 2.28 shows a section cut halfway between two cracks. The average tensile stress transverse to the struts is f_1, which gives rise to a vertical force equal to $f_1 \cdot b_w \cdot d_v \cdot \cot g\theta$. As the two sets of stresses shown in Figures 1.b and 1.c must equilibrate the same vertical shear in both cases, we see that

$$V_c = \upsilon_{ci} b_w d_v = f_1 b_w d_v \cot g\theta \tag{2.42}$$

thus,

$$f_1 = \upsilon_{ci} \tan\theta \tag{2.43}$$

Therefore, after the stirrups yield the beam will not collapse if the shear friction increases and the angle θ decreases. The failure of the beam is governed by the crushing of the compression struts between the cracks, or by the crack slip. The stress, f_2, in a compression strut is given by

$$f_2 = f_1 - \upsilon(\tan\theta + \cot\theta) \tag{2.44}$$

The concrete is subjected to normal tensile stresses, and as the principal tensile strain, ε_1, increases, the maximum compressive strength decreases.

Therefor, after the stirrups yield, the shear strength of a concrete beam can be increased. Generally, for a normal strength concrete beam, the crushing of the concrete governs the beam failure. In a high-strength concrete beam, the struts are able to carry more compressive stress, and failure is most likely initiated by the crack slip.

Finally, it is important to highlight the main differences between the truss model and the MCFT concrete contributions:

- The truss model concrete contribution is considered equal to the shear strength of a similar beam without shear reinforcement. The MCFT takes into account a concrete contribution based on the actual collapse mechanism of a reinforced concrete beam.

- The truss model concrete contribution does not vary with the amount of transverse reinforcement. The MCFT concrete contribution depends on the crack width. The more shear reinforcement, the lesser the crack width, and the greater the concrete contribution will be.

2.3.6 Code review

Spanish Code EHE-99

The EHE code of practice assumes that a concrete contribution, V_c, can be added to the steel contribution. Hence

$$V = V_s + \beta V_c \tag{2.45}$$

and

$$V_c = \left[0.10\left(1+\sqrt{\frac{200}{d}}\right)\left(100\rho_s f_{ck}\right)^{1/3} - 0.15\sigma'_{cd} \right] b_0 d \tag{2.46}$$

where all the parameters have the same meaning as for members without web reinforcement (equation 2.6). The steel contribution is given by the following equation:

$$V_s = \frac{A_{sw}}{s} z\, f_{ywd}\, \cot\theta \tag{2.47}$$

where $\cot\theta$ is compressed between 0.5 and 2. For non-prestressed members without axial force β equals 1 if θ is taken to be 45°. If $\cot\theta$ is assumed to be equal to 2 (thus, $\theta \approx 26.6°$), then $\beta = 0$.

Eurocode 2: April 2002 Final Draft

For members requiring design shear reinforcement, their design is based on a truss model. For members with vertical shear reinforcement, the shear resistance, $V_{Rd,s}$, should be taken to be the lesser, either:

$$V_{Rd,s} = \frac{A_{sw}}{s} z\, f_{ywd}\, \cot\theta \tag{2.48}$$

or

$$V_{Rd,max} = \alpha_c b_w z \nu f_{cd} / \left(\cot\theta + \tan\theta\right) \tag{2.49}$$

The recommended limiting values for $\cot\theta$ are given by the expression

$$1 \le \cot\theta \le 2.5 \tag{2.50}$$

where

A_{sw} is the cross-sectional area of the shear reinforcement,

s is the spacing of the stirrups,

f_{ywd} is the yield strength of the shear reinforcement,

ν may be taken to be 0.6 for $f_{ck} \leq 60$ MPa, and 0.9-f_{ck}/200 for high-strength concrete beams and

α_c = 1, for non-prestressed structures.

AASHTO LFRD 2000

The shear strength of a reinforced concrete section is expressed as follows

$$V_n = \beta \sqrt{f_c'} b_v d_v + \frac{A_v f_y}{s} d_v \cot\theta \tag{2.51}$$

The values of β and θ listed in Figure 2.29 are based on a calculation of the stress that can be transmitted across diagonally-cracked concrete containing at least the minimum amount of transverse reinforcement required for crack control.

The shear stress in Figure 2.29 can be defined as

$$\nu = \frac{V_n - V_p}{b_v d_v} \tag{2.52}$$

For members with stirrups ε_x can be taken to be 0.5·ε_t, as is demonstrated in Figure 2.29. ε_t is calculated using equation 2.11.

ACI Code 318-99

For members requiring design shear reinforcement, their design is based on a 45º truss model plus a concrete contribution. Hence

$$V = V_c + V_s \tag{2.53}$$

and

$$V_{Rd,s} = \frac{A_{sw}}{s} z f_{ywd} \tag{2.54}$$

and the concrete contribution is equal to the failure shear strength of an identical beam without web reinforcement, given by equation 2.13.

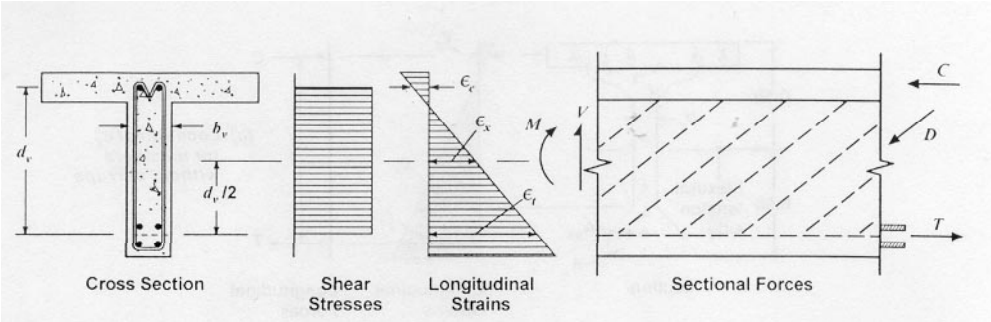

$\frac{\nu_f}{\phi_c f'_c}$		$\varepsilon_x \times 1000$					
		≤ 0.00	≤ 0.125	≤ 0.25	≤ 0.50	≤ 0.75	≤ 1.00
≤ 0.075	β θ	0.311 21.8	0.269 24.3	0.244 26.6	0.215 30.5	0.198 33.7	0.185 36.4
≤ 0.100	β θ	0.261 22.5	0.242 24.9	0.228 27.1	0.208 30.8	0.193 34	0.181 36.7
≤ 0.125	β θ	0.238 23.7	0.228 25.9	0.218 27.9	0.201 31.4	0.188 34.4	0.177 37
≤ 0.150	β θ	0.226 25	0.216 26.9	0.209 28.8	0.196 32.1	0.184 34.9	0.173 37.3
≤ 0.175	β θ	0.21 26.26	0.209 28	0.203 29.7	0.189 32.7	0.178 35.2	0.163 36.8
≤ 0.200	β θ	0.208 27.4	0.202 29.0	0.197 30.6	0.178 32.8	0.161 34.5	0.149 36.1
≤ 0.225	β θ	0.199 28.5	0.194 30.0	0.178 30.8	0.154 32.3	0.144 34.0	0.136 35.7
≤ 0.250	β θ	0.178 29.7	0.176 30.6	0.160 31.3	0.141 32.8	0.131 34.3	0.125 35.8

Figure 2.29: Values of β and θ for sections containing at least the minimum amount of shear reinforcement.

2.4 Shear strength in high-strength concrete beams

2.4.1 Introduction

As far as shear strength is concerned, Duthinh et al. (1996) asses that high-strength concrete presents us four main challenges:

- Current code provisions for shear strength design rely on empirical rules whose database is largely below 40 MPa. New design rules would have to rely on either rational methods or on tests that cover a higher range of strengths. Much progress has been made in the last 25 years on rational methods for shear design and there is hope that the rules can be made more understandable from first principles of mechanics, such as has been achieved

for flexure. Moreover, it is likely that the rules can be made simple enough that they will gain adoption by the design community in the not-too-distant future.

- Shear failure surfaces in high-strength concrete members are smoother than in normal-strength concrete members, with cracks propagating through coarse aggregate particles rather than around them (Figure 2.30). Since one of the shear transfer mechanisms across cracks is by aggregate interlock, this mechanism needs to be re-examined for high-strength concrete. Test results to date indicate that shear friction in HSC can be as low as 35% of that in NSC (Walraven, 1995).

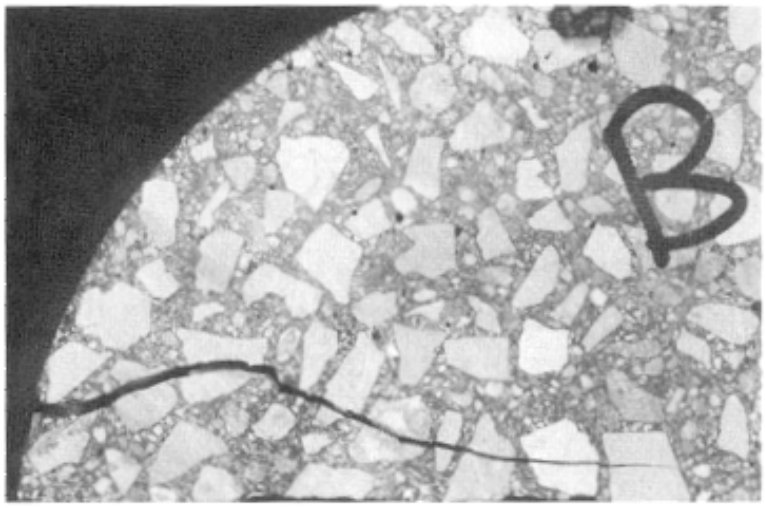

Figure 2.30: Crack in high-strength concrete

- In the cracked web of a beam under shear, the portions of concrete between cracks act as compression struts that are also subjected to transverse tension, which reduces their compression capacity. Modelling of this softening behaviour is based on tests. Softening shows a dependence on concrete strength that needs to be extended to HSC. However, test results to date indicate no marked difference in biaxial tension-compression behaviour between HSC and NSC.

- Minimum shear reinforcement must prevent sudden shear failure on the formation of first diagonal tension crack and, in addition, must adequately control the diagonal tension cracks at service load levels. To prevent a brittle

failure, an adequate reserve of strength must be provided by the shear reinforcement after diagonal cracking of reinforced concrete beams. To control crack widths at service load levels, not only must a minimum amount of shear reinforcement be provided, but the maximum stirrup spacing must also be limited. Due to the higher tensile strength of high-strength concrete, a higher cracking shear is expected and hence, would require a larger amount of minimum shear reinforcement (Yoon et al., 1996).

2.4.2 Minimum web reinforcement

Shear failure in a beam without web reinforcement is sudden and brittle. Therefore, it is necessary to provide a minimum amount of shear reinforcement, which must prevent sudden shear failure on the formation of first diagonal tension cracking and, in addition, must adequately control the diagonal tension cracks at service load levels.

Thus, the minimum area of web reinforcement is intended to ensure that the capacity of the member after cracking exceeds the load at which inclined cracking occurs. For some member types, such as slabs and footings, this requirement may be waived because load redistribution can occur across the width of the member.

Johnson and Ramirez (1989) studied the minimum shear reinforcement in beams with high-strength concrete. From an evaluation of the results of this experimental investigation and previous studies, it was concluded that the overall reserve shear strength after diagonal tension cracking diminished with the increase in f'_c for beams with the same minimum amount of shear reinforcement.

Roller and Russell (1990, based on an experimental investigation of 10 beams, proposed a new amount of minimum reinforcement for high-strength concrete beams, as the ACI equation was unconservative.

More recently, the Spanish EHE code of practice proposed that the minimum area of web reinforcement must confirm that

$$\sum \frac{A_\alpha f_{y\alpha,d}}{\sin\alpha} \geq 0.02\, f_{cd}\, b_0 \tag{2.55}$$

where A_α is the area of web reinforcement per length unit inclined an angle α from the longitudinal axis of the beam; $f_{y\alpha,d}$ the factored yield strength of the transverse reinforcement, inclined α degrees; and f_{cd} the factored compression strength of the concrete.

However, this expression is very conservative when f_c increases, as the first diagonal tension cracking is not proportional to the compression strength of the concrete. Tests suggest that the inclined cracking load of beams increases proportionally with the tensile strength of the concrete.

The *Concrete Society Technical Report 49* (1998) proposed the next equation in the 'Design guidance for high-strength concrete':

$$A_{sv} \geq 0.4 \left(\frac{f_{cu}}{40} \right)^{2/3} \frac{b_v s_v}{0.95\, f_{yv}} \tag{2.56}$$

where A_{sv} is the area of the web reinforcement, s_v the stirrup spacing, f_{yv} the yield strength of the transverse reinforcement, and f_{cu} the cubic compressive strength of the concrete. The 'Design guidance for high-strength concrete' defines f_{cu} as the lesser: $1.25f_c$ or f_c + 15 MPa.

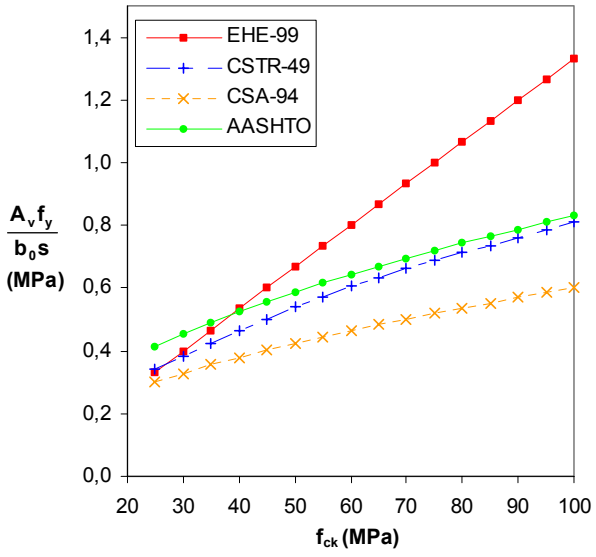

Figure 2.31: Comparison of minimum web reinforcement provisions.

The AASHTO LFRD Specifications propose a minimum amount of web reinforcement given by the following equation

$$A_v \geq 0.083\sqrt{f'_c}\frac{b_w s}{f_y} \tag{2.57}$$

Yoon, Cook and Mitchell (1996) carried out an experimental campaign on minimum shear reinforcement in normal, medium and high-strength concrete. Twelve shear tests were conducted. It was shown that the CSA-94 provisions, shown in equation 2.58, give enough reserve of resistance.

$$A_v \geq 0.06\sqrt{f'_c}\frac{b_w s}{f_y} \tag{2.58}$$

This equation was revaluated in 1999 by Ozcebe et al. (1999). They concluded, based on 13 tested beams, that the amount given in the previous equation could be 20% smaller. However, it is necessary to recall the difference in beam depth from one experimental campaign to the other. Yoon et al. tested 750 mm deep beams, compared with the 360 mm specimens tested by Ozcebe et al. (1999)

The above equations provide very different amounts of web reinforcement, as plotted in Figure 2.31, the difference being greater when the concrete compression strength is higher.

2.4.3 Shear strength in HSC beams without web reinforcement

Most of the research in recent years has intended to evaluate the shear strength of high-strength concrete beams without web reinforcement.

In 1984, Mphonde and Frantz tested 3 series of reinforced concrete beams with nominal concrete compressive strengths ranging from 21 to 103 MPa. Within each series the shear span-depth ratio was held constant at either 3.6; 2.5; or 1.0. Test results indicated that for slender beams the accuracy of the ACI beam shear strength equations varies

greatly with the concrete strength. Furthermore, the effect of the concrete strength on the shear capacity becomes more significant as the beams become shorter.

Ahmad, Khaloo and Poveda (1986) tested thirty-six reinforced concrete beams using 65 MPa concrete. None of the beams had shear reinforcement and half of them had an *a/d* ratio greater than 2.5. They concluded that the current ACI Code could be unconservative for high-strength concrete beams with a low percentage of longitudinal steel, as will be discussed in Chapter 5.

Also in 1986, Elzanaty, Nilson and Slate (1986) carried out an experimental study of the shear strength of reinforced concrete beams made using concrete with compressive strengths ranging from 21 to 83 MPa. A total of 18 beams were tested. Their conclusions were very similar to those of Ahmad et al.

Some years later, between 1990 and 1995, Ahmad et al. carried out several experimental campaigns to evaluate the shear strength of reinforced lightweight concrete beams made of normal and high-strength concrete with and without shear reinforcement. The results indicated that the predicted ultimate shear capacities, in accordance with the ACI Code and the BS 8110 Code, provide an adequate margin of safety when compared with the observed values for normal as well as high-strength lightweight concrete beams using different types of lightweight aggregates such as stalite, lytag, pellite and pumice.

In Norway, Thorenfeldt and Drangsholt (1990) tested 28 reinforced concrete beams without shear reinforcement in shear by two-point loading. For members made of concrete with $f'_c > 80$ MPa, the diagonal cracking strength remained largely constant, with a minor decrease, in spite of the increasing tensile strength of the concrete. Surprisingly, the ultimate shear strength decreased as the concrete compressive strength increased above 80 MPa, probably because of the increasing brittleness due to the increase in strength (Duthinh et al., 1996).

Kim and Park (1994) carried out a experimental campaign testing 20 beam specimens whose concrete compressive strengths were around 54 MPa. They concluded that the MC-90 equation predicts the shear strength relatively well and that the ACI equation is

unsafe for large beams. They also determined that the effect of size on shear strength was the same for normal-strength and high-strength concrete.

However, Collins and Kuchma (1999) published the results of an extensive experimental investigation aimed at evaluating the significant parameters which influence the size effect in shear. It was found that the reduction in shear stress at failure was related more directly to the maximum spacing between the layers of longitudinal reinforcement rather than the overall member depth. Moreover, high-strength concrete beam specimens showed a more significant size effect in shear than normal-strength concrete members. Angelakos, Bentz and Collins (2001) determined that for members without stirrups, the shear stress at failure can decrease substantially as the members become larger and as the longitudinal reinforcement ratio decreases.

In 2002, Fujita et al. (2002) demonstrated that the size effect on the shear capacity is linked to the concrete compressive strength. Experimental tests they carried out showed that shear fracture in HSC is characterised by a conspicuous localisation of cracking in comparison with ordinary strength concrete, and that the propagation of these cracks was rapid, resulting in a more brittle fracture. A study using Fracture Mechanics was conducted by Fujita et al. to determine the relationship between size effect and concrete compressive strength, leading to the expressions shown in §5.4.3.

2.4.4 Shear strength in HSC beams with web reinforcement

Most research on shear strength in HSC beams has dealt with the minimum amount of web reinforcement, as has been presented in §2.4.2. The number of experimental campaigns with higher amounts of web reinforcement is not as high as the number of studies on beams without web reinforcement.

In 1986, Elzanaty et al. (1986) tested three beams with web reinforcement. One of them was made of high-strength concrete. According to their tests, the use of HSC tends to prevent shear-compression failure and to ensure a diagonal tension failure instead, thus increasing the effectiveness of shear reinforcement (Duthinh et al., 1996)

In Spain, Aparicio, Calavera and Del Pozo (1997) tested seven full-scale prestressed and reinforced precast beams to study the crushing of the web. They also developed a strut and tie model with arch effect. The author is unaware of any other research that has been carried out in Spain on high-strength concrete beams failing on shear after the yielding of the stirrups.

Fourteen HSC beams failing in shear were tested by Sarsam and Al-Musawi (1992), and Kong and Rangan (1998) tested 48 reinforced high-performance concrete beams with vertical shear reinforcement under combined bending moment and shear with *a/d* ratios ranging from 1.51 to 3.60. They also reported the results of a statistical analysis performed on 147 earlier test results. Both Sarsam et al. and Kong et al. concluded that a large coefficient of variation was obtained when HSC test beam results were compared with the predictions made by various code provisions.

The effect of concrete strength and minimum stirrups on shear strength of large members was studied by Angelakos in his doctoral thesis in 1999, which was later published by Angelakos, Bentz and Collins (2001). The experiments indicated that even members containing 16% more than the minimum amount of stirrups specified by the ACI Code will still have inadequate margins of safety.

2.5 Conclusions of the state-of-the-art

Since the beginning of the 20th century, when Mörsh and Ritter postulated the earliest truss models, great progress has been made in the analytical solution of shear problems in reinforced concrete. However, most of these highly sophisticated tools require considerable simplification to make them suitable for codes of practice. Moreover, as Regan (1993) points out, the most imposing analyses have often shown an excellent correlation with known results but have failed to predict behaviour under untested circumstances. For simpler models the problems is mostly that of the need to neglect secondary factors, yet what is secondary in one case may be primary in another, so very careful confirmation is always needed. Further progress will no doubt be achieved, especially in the simplification of analytical methods and in D-regions, as the exactness of the solutions available for B-regions far surpasses those for disturbed regions.

It is the author's opinion that the EHE procedure should be improved in coming years. The minimum amount of shear reinforcement provided by the Spanish code of practice may be suitably reduced as concrete strength increases.

For members without web reinforcement, the current EHE procedure predicts the test results reasonably well, as will be shown in Chapter 5. However, the decrease in shear strength for high-strength concrete members without web reinforcement has not been solved in any code of practice procedure.

For members with web reinforcement, the lack of physical evidence for taking a concrete contribution into account in a beam with stirrups equal to (or 85% of) the same beam without transverse reinforcement should be corrected. The AASHTO procedure, based on the MCFT, presents a more rational approach than the EHE or Eurocode, although it is certainly more complex than traditional procedures.